

# Screen-printed graphite macroelectrodes for the direct electron transfer of cytochrome c: a deeper study of the effect of pH on the conformational states, immobilization and peroxidase activity

Cite this: *Analyst*, 2014, **139**, 1442Maria Gómez-Mingot,<sup>†a</sup> Vicente Montiel,<sup>a</sup> Craig E. Banks<sup>\*b</sup> and Jesús Iniesta<sup>\*a</sup>

The direct electron transfer of cytochrome c has been studied at screen-printed graphite macroelectrodes without recourse to mediators or the need for any electrode pre-treatment as is commonly employed within the literature. A wide range of pH values from 2.0 to 11.0 have been explored upon the electrochemical response of cytochrome c and different voltammetric signatures have been observed. The direct electron transfer of the alkaline transition of cytochrome c was found impeded within alkaline media leading to either an irreversible redox process or even no voltammetric responses. In acidic aqueous media the electrochemical process is observed to undergo a mixed diffusion and adsorption controlled process rather than a purely diffusional process of the native conformation as observed at pH 7.0. Interestingly, at pH 3.5 a new conformational state is revealed in cooperation with the native conformation. The immobilization of the protein was satisfactorily obtained using a simple method by cycling the protein at specific solution pH values allowing amperometric responses to be obtained and gives rise to useful *pseudo*-peroxidase activity for sensing H<sub>2</sub>O<sub>2</sub>. Apparent Michaelis–Menten constant values ( $K_m$ ) were calculated *via* the Lineweaver–Burk method with deduced values of  $25 \pm 4$ ,  $98 \pm 12$  and  $230 \pm 30$  mM, respectively for pH values of 2.0, 3.0 and 7.0. Such work is important for those utilising cytochrome c in bio-electrochemical and related applications.

Received 18th November 2013  
Accepted 22nd December 2013

DOI: 10.1039/c3an02137h

www.rsc.org/analyst

## 1. Introduction

Structural changes and dynamics of intermolecular electron transfer (ET) in native cells are responsible for addressing cell membrane processes such as ion pump regulation, electric field-related treatment, ion-transport channel functioning across membranes and protein–protein interactions.<sup>1,2</sup> Thus, characterization studies of proteins' structural changes and their immobilization upon surfaces are vital as a means of constructing a biomimetic system able to reproduce biological mechanisms.

Cytochrome c (cyt-c) is a membrane protein responsible for the ET in the transport chain and it may exist in solution in five reversible, pH-dependent conformational states with  $pK_a$  values

of 0.42, 2.50, 9.35, and 12.76, denoted as states: I, II, III, IV, and V, respectively.<sup>3,4</sup> The iron in the native *heme* of the protein is complexed within the porphyrin axially to a methionine (*Met80*) and a histidine (*His18*), while it is covalently attached *via* thioether bonds to the polypeptide backbone throughout two cysteine residues (*Cys14* and *Cys17*). Two factors make the reduction potential of the native (N) state of cyt-c (state III – ~unusually positive values of +0.2 V to +0.38 V). The first is the stabilization effect of the Fe(II) state due to the  $\pi$ -electron accepting character of the thioether sulphur atom of *Met80* and the second is the inaccessibility to the *heme* which is buried within a hydrophobic pocket, which also favours the ferrous state beyond the ferric.<sup>5</sup>

Non-native states of cyt-c have been studied in depth as they have a role, not fully understood, in apoptosis and cellular oxidative stress processes beyond the ET function.<sup>6,7</sup> The effects on the protein stability and structure and furthermore the influence on the *heme* coordination due to changes of pH, anionic strength and nature of the anions have been widely and extensively studied.<sup>8,9</sup> In this respect, the alkaline isomerisation is known as the transition of cyt-c from neutral pH (state III) to alkaline pH (state IV) and results from the disruption of the *Met80*–Fe coordination bond and the introduction of a residue of lysine (*Lys72*). The other main covalent transition occurs at

<sup>a</sup>Physical Chemistry Department and Institute of Electrochemistry, University of Alicante, 03690 San Vicente del Raspeig, Alicante, Spain. E-mail: [jesus.iniesta@ua.es](mailto:jesus.iniesta@ua.es); Fax: +34 965903536; Tel: +34 965909850

<sup>b</sup>Faculty of Science and Engineering, School of Science and the Environment, Division of Chemistry and Environmental Science, Manchester Metropolitan University, Chester Street, Manchester M1 5GD, Lancs, UK. E-mail: [c.banks@mmu.ac.uk](mailto:c.banks@mmu.ac.uk); Fax: +44 (0) 1612476831; Tel: +44 (0)1612471196

<sup>†</sup> Present address: Nano-Electrochemistry Group, Université Paris Diderot, Sorbonne Paris Cité, ITODYS, UMR 7086 CNRS, 15 rue Jean-Antoine de Baïf, 75205 Paris Cedex 13, France.



acidic pH values with the formation of the low-pH conformer (state II,  $pK_a \sim 2.5$ ) in which both axial ligands are protonated and detached from the iron, thus conforming a high spin configuration, in which axial positions are occupied by water molecules. Moreover, it has been reported that an intermediate state is formed during the process of total unfolding of the protein by the *Met80*-Fe disruption (state II). This stable state is caused by a non-covalent modification and is called the molten globule state (MG) which has a  $pK_a \sim 3.0$ .<sup>10</sup> As explained, there are plenty of stable conformations of the protein depending on the pH value, and it is thought that the relationship of the differences between kinetic intermediates and the equilibrium of the MG state could probably be the key for the protein unfolding and refolding.<sup>11–13</sup>

Interfacial interactions of ET between proteins and electrochemical platforms are widely studied with the aim of providing insight into *in vivo* behaviour which can be exploited in bio-electrocatalytic systems.<sup>14,15</sup> Functionalities residing at the carbon electrode surfaces, usually upon edge plane like-sites/defects, ensure favourable electrostatic interactions with proteins. Studies on cyt-c immobilization on a surface of a basal plane graphite electrode in a room temperature ionic liquid,<sup>16</sup> on silicon dioxide nanoparticles-modified electrodes,<sup>17</sup> and on clay colloidal-membranes<sup>18</sup> obtained clear direct ET. Recently, we have demonstrated that screen-printed graphite electrodes (SPGEs) provide direct ET for cyt-c in aqueous solutions due to the electrostatic interaction between the positively charged Lys amino groups on cyt-c and the negatively charged carboxylated groups on the surface of the electrode.<sup>19</sup> The negative charge density of the surface depends on the solution pH, and hence the pH dependence of the ET rate is attributed to changes in the rearrangement reaction rate of cyt-c on the electrode surface. However, to the best of our knowledge the pH effect of solutions on the cyt-c conformation and hence their ET characterization of different conformational states has not yet been examined on graphitic surfaces in SPGE platforms.

In this work, we employ electrochemical techniques to study the pH-dependent dynamics of the direct charge-transfer processes of cyt-c using SPGEs in a very wide range of pH values, from 2.0 to 11.0. Immobilization of cyt-c is induced by electrochemical cycling at different pH solutions and an average coverage of protein is determined with different solution pH values. Furthermore, in order to investigate the peroxidase activity of the adsorbed redox protein towards  $H_2O_2$ , the addition of increasing concentrations of this oxidizing agent resulted in the calculation of the apparent Michaelis–Menten kinetic constant.

## 2. Materials and methods

### 2.1. Materials

All chemicals used were of analytical grade and were used as received without any further purification. All solutions were prepared with deionised water of resistivity not less than 18.2 M $\Omega$  cm (Millipore, Merck, Germany). Cyt-c from horse skeletal muscle (Sigma,  $\geq 95\%$ ) was used as received. The supporting electrolyte for the solutions of cyt-c was 0.1 M  $NaH_2PO_4$  (PBS,

Sigma) which gave a pH of 4.33; this solution was acidified with the addition of *o*- $H_3PO_4$  (85 wt%, Sigma) to obtain solutions in the pH range of 2.0 up to 4.0 and basified with the addition of NaOH (Sigma) to obtain solutions with pH values greater up to 11.0.  $H_2O_2$  solutions of 200 mM were prepared freshly in the convenient PBS pH value solution from dilution of  $H_2O_2$  (50 wt%, Sigma).

### 2.2. Cyclic voltammetry

Voltammetric measurements were carried out using a  $\mu$ -Autolab III (Eco Chemie, The Netherlands) potentiostat/galvanostat and controlled by Autolab GPES software version 4.9 for Windows XP. All measurements were carried out using a three-electrode configuration where the working (3.1 mm diameter) and counter electrodes consist of carbon with a silver/silver chloride reference electrode (*pseudo*Ag/AgCl). The carbon-based screen printed electrodes were fabricated in-house with appropriate stencil designs using a microDEK 1760RS screen-printing machine (DEK, Weymouth, UK). First, a carbon-graphite ink formulation (Product Code: C2000802P2; Gwent Electronic Materials Ltd, UK) was screen-printed onto a polyester (Autostat, 250 micron thickness) flexible film. This layer was cured in a fan oven at 60 degrees for 30 minutes. Next a silver/silver chloride reference electrode was included by screen printing Ag/AgCl paste (Product Code: C2040308D2; Gwent Electronic Materials Ltd, UK) onto the polyester substrates. Finally, a dielectric paste (Product Code: D2070423D5; Gwent Electronic Materials Ltd, UK) was then printed onto the polyester substrate to cover the connections. After curing at 60 degrees for 30 minutes the screen-printed electrodes are ready to be used. Studies involving the scan rate were performed with a solution of 0.08 mM of cyt-c in different pH values. The experimental set-up was very simple as these studies were performed in a drop covering the SPGE surface. For comparison, formal potentials of the ET of cyt-c ( $E^0$ , expressed in mV) subjected to pH variations were referred to a standard reference electrode Ag/AgCl/KCl (3.5 M). Experiments were carried out at room temperature.

### 2.3. Adsorption of cyt-c

A forced adsorption procedure of cyt-c on the SPGEs was electrochemically performed cycling between +0.2 and –0.2 V (*vs.* *pseudo*Ag/AgCl) at 100 mV s<sup>–1</sup> for 100 cycles the SPGE in different PBS buffer solutions containing a protein solution concentration of 0.162 mM at room temperature and at the desired pH value. After adsorption, the SPGE was gently rinsed with Millipore water and rapidly covered with buffer PBS solution to further study the peroxidase activity.

### 2.4. Cyt-c peroxidase activity study

After performing the cyt-c adsorption procedure at pH 2.0, 3.0, 4.0 and 7.0 the electrode was immersed into a PBS solution (2 mL volume cell) and waited for stabilisation of the baseline. Chronoamperometry was performed at a cathodic potential of –0.5 V (*vs.* *pseudo*Ag/AgCl) under mass control conditions using a magnetic bar at constant stirring. Baseline corrections regarding the electrochemical reduction of  $H_2O_2$  in the absence



of cyt-c adsorbed onto the SPGE platform were performed for all experiments.

### 3. Results and discussion

#### 3.1. Influence of solution pH value on the electrochemistry of cyt-c/SPGE

The pH-dependent voltammetric signatures of 0.08 mM cyt-c at SPGEs were first explored over a wide pH range from 2.0 to 11.0, as depicted in Fig. 1, where Fig. 1A shows the response for pH values between 2.0 and 3.0, Fig. 1B shows the response between pH 3.5 and 5.0, Fig. 1C shows the response between pH 6.0 and 8.0 and, finally, Fig. 1D shows the response between pH 9.0 and 11.0.

Our previous work demonstrated that well-defined and quantifiable voltammetric responses are readily observed at physiological pH using screen-printed electrodes.<sup>19</sup> Any variation of the solution pH would induce conformational changes at the protein and would resonate the active site since the redox centre of cyt-c is embedded within a rigid 34 Å diameter shell with nine positive charges at pH 7.0 with a considerable dipole moment.<sup>20–23</sup> At pH 7.0 the dominant state of cyt-c is III (*His18* and *Met80* in axial positions of the *heme*),<sup>24,25</sup> whereas at pH close to  $pK_a$  9.5 a conformational transition occurs between states III and IV which involves the substitution of *Met80* from the *heme*, presumably by *Lys79*.<sup>26</sup> The progressive loss of voltammetric ET at alkaline pH values (Fig. 1C) could be correlated with the de-coordination of the axial *His18* and *Met80* ligands in the *heme* pocket. The conversion of cyt-c due to variation of pH

from extreme values (Fig. 1A) reflects a remarkable effect on the ET kinetics and activity of the protein.

Cyclic voltammograms (CVs) presented in Fig. 1 are analysed in terms of the peak potential separation ( $\Delta E_p$ ), formal potential ( $E^0$ ) and ET rate constant ( $k_s$ ) with variation of pH (Fig. 2). As a summary, Fig. 2 shows the dependence of these parameters upon pH where the  $\Delta E_p$  values remain almost unchanged as it ranges from 30 mV (at 50  $\text{mV s}^{-1}$ ) at pH 2.0 to 75 mV at pH 7.0 (Fig. 2A), whereas the  $E^0$  ranges from 235 mV (vs. standard Ag/AgCl/KCl (3.5 M)) at pH 2.0 to 174 mV (vs. standard Ag/AgCl/KCl (3.5 M)) at pH 7.0 (Fig. 2B). In alkaline solutions above pH 8.0, the shape of the peak broadens,  $\Delta E_p$  is enlarged (Fig. 2A) and barely non-defined redox peaks are obtained (Fig. 1D). The direct ET rate constant ( $k_s$ ) was calculated according to the method described by Laviron<sup>27</sup> for mixed diffusion and adsorption processes and under experimental conditions with  $\Delta E_p$  smaller than 200 mV and assuming that the number of electrons in the process is  $n = 1$  and the charge-transfer coefficient  $\alpha$  is 0.5 for 50  $\text{mV s}^{-1}$ . Fig. 2B shows that the  $k_s$  value at pH 7.0 was 0.7  $\text{s}^{-1}$ , while a decrease in  $k_s$  values is clearly observed at high pH values as denoted by a more irreversible ET process, 0.5  $\text{s}^{-1}$  at pH 8.0. In contrast,  $k_s$  values increase at lower pH values, leading for example to values of 2.4  $\text{s}^{-1}$  and 1.1  $\text{s}^{-1}$  at pH 2.0 and 3.5, respectively. As stated before, Fig. 2B correlates very well the variation of the  $\Delta E_p$  with ET rate  $k_s$  along pH. Furthermore, Fig. 2C shows how the  $I_{pc}/I_{pa}$  ratio varies with pH with a tendency towards 1.0 at pH values ranging from 2.0 to 7.0, whereas it shows a minimum value of 0.5 at pH 3.5. Similarly, the effect of scan rate ( $\nu$ ) was explored over the range from 1 to 1000  $\text{mV s}^{-1}$  showing two clear tendencies to linearity of plots regarding anodic and cathodic peak currents ( $I_{pa}$  and  $I_{pc}$ , respectively, results not shown). In the pH range between 2.0

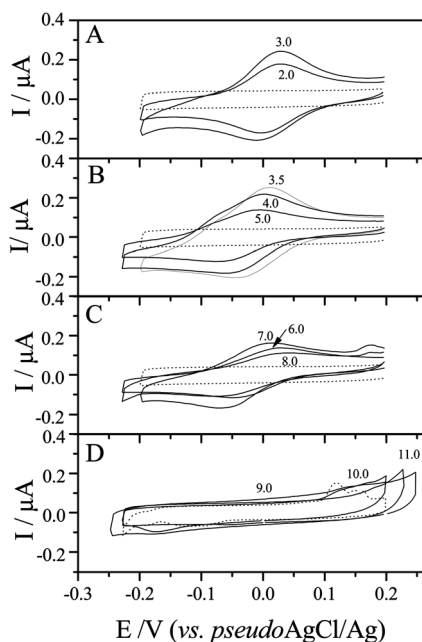


Fig. 1 Cyclic voltammetric profiles of 0.08 mM cyt-c/SPGE in 0.1 M PBS at different pH values: (A) 2.0 and 3.0, (B) 3.5, 4.0 and 5.0, (C) 6.0, 7.0 and 8.0 and (D) 9.0, 10 and 11.0. Data were obtained from the CVs at 50  $\text{mV s}^{-1}$ . The dotted line is related to the PBS background response.

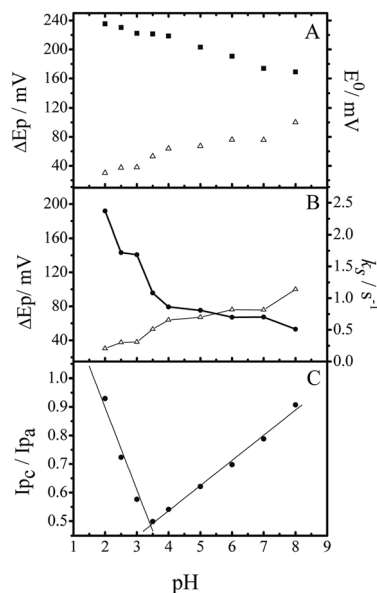


Fig. 2 Dependence of current intensity peak separation ( $\Delta E_p/\text{mV}$ , open triangles) and formal potential ( $E^0/\text{mV}$ , dark squares) over pH (A), the ET constant variation ( $k_s/\text{s}^{-1}$ , dark circles) vs. pH (B) and  $I_{pc}/I_{pa}$  ratio vs. pH (C). Data obtained for 50  $\text{mV s}^{-1}$ .



and 3.5 plots of  $I_{pa}$  and  $I_{pc}$  against scan rate are found to be linear ( $R^2 = 0.995$ ) denoting a predominance of the adsorption-controlled process while in the pH range between 4.0 and 8.0 a linearity towards the square-root of the scan rate is displayed which is indicative of a purely diffusion-controlled process.

Under extreme acidic conditions (pH 2.0), the electrochemical response of the protein shows a clear oxidation–reduction profile. Parameters obtained from the voltammetric signatures such as  $\Delta E_p$  and  $E^{0'}$  were similar for pH values of 2.0 and 3.0. This indicates that our experimental conditions of buffer solution concentration (0.1 M PBS) kept substantially almost unaltered the *heme* surrounding conformation and therefore the protein is not denaturalised at pH 2.0.<sup>28,29</sup> As shown above, with the increase of the solution pH from 2.0 to 8.0,  $E^{0'}$  shifted very slightly to lower values giving a variation of 65 mV. Moreover, it is remarkable that the peak current ratio ( $I_{pc}/I_{pa}$ ) – extracted from Fig. 1 – showed a minimum value of 0.5 at pH 3.5 which would be in agreement with the plausible explanation that two species in equilibrium are being oxidised. Thus, considering that carboxylic groups on the electrode surface with  $pK_a$  values near to 4.5, acidic pH values up to 5.0 provided a neutral protonated surface. This protonated surface interacts with positively charged amino residue groups in the protein, whereas at pH values higher than 5.0 and when the protein isoelectric point –  $pI$  10.5 – is reached the carboxylated groups on the surface start to compensate the  $-\text{NH}_3^+$  groups and the repulsive charges between negatively charged surface and global negative charge of the protein makes the interfacial ET processes unviable.

The presence of a single species adsorbed on the electrode is evidenced as being in the native form (N), which is oxidised and reduced on the electrode surface, and another species is observed when the pH is decreased to a value near 3.5. In that respect and close to these pH values – between 3.0 and 4.0 – two cathodic and anodic peaks are revealed at low scan rates, whilst at moderately higher scan rates a small shoulder can be discerned around +0.1 V. Fig. 3 shows the simultaneous and direct ET responses for N and another acidic-dependent species with a different conformational state for different pH values, 2.5 (Fig. 3A), 3.0 (Fig. 3B), 3.5 (Fig. 3C), and 4.0 (Fig. 3D) at low scan rates ( $1 \text{ mV s}^{-1}$ ). Similarly, for the oxidation process I–O, the peak potential remains almost constant at pH values of 2.5 and 3.0 with  $E_p$  close to 50 mV whereas at pH 3.5 and 4.0 the  $E_p$  decreased to a value of 28 mV. Nevertheless,  $\Delta E_p$  resulted to be close to the theoretical *ca.* 59 mV for one electron process. The presence of a new slightly-defined reduction peak (II–R) is revealed at pH 3.5 and becomes clearer at pH 4.0 at a peak potential of about –144 mV and –154 mV, respectively. At the same time, at these pH values, the most striking characteristic of this study was the second oxidation peak (II–O) which appeared at –90 mV, and most remarkably the  $\Delta E_p$  for both processes I and II resulted to be approximately 54 mV at pH 3.5. However, at pH 4.0,  $\Delta E_p$  could be estimated to be *ca.* 67 mV for process I and *ca.* 62 mV for process II. Moreover, under deoxygenated conditions, the electrochemical behaviour of cyt-c at pH 2.5, 3.0, 3.5 and 4.0 gave rise to the same CV trace as that described in Fig. 3 discarding that these two peaks were related to the electrochemical reduction of oxygen.

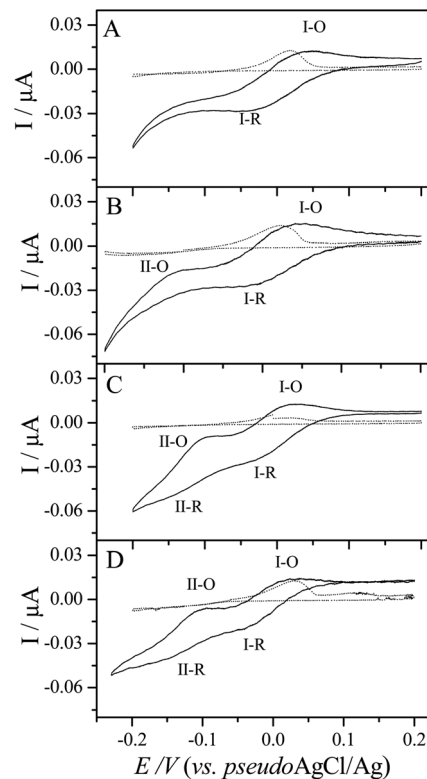


Fig. 3 Cyclic voltammetric profiles of 0.08 mM cyt-c/SPGE in 0.1 M PBS at different pH values: 2.5 (A), 3.0 (B), 3.5 (C) and 4.0 (D) recorded at  $1 \text{ mV s}^{-1}$ . The dotted line is related to the PBS background response.

As shown in Fig. 1B and further observed when applying a slow scan rate (Fig. 3), a pH-dependent acidic protein conformation which is in equilibrium with the cyt-c N state is revealed and hypothesized as the MG state. The MG state has a compact secondary structure and a largely disordered tertiary structure which lacks well-packed side chains but retains the hydrophobic core as in the N state.<sup>10,12</sup> The most remarkable fact was the observation of a “second” anodic peak (II–O) at a peak potential of –0.1 V (Fig. 3C).

### 3.2. Electrochemical properties of cyt-c immobilized on SPGE

The structure conformation of cyt-c is also intimately related to immobilization of cyt-c onto the SPGE platform. At acidic pH the peak current ( $I_p$ ) showed a linear response as a function of scan rate, denoting an adsorption-controlled process. Conformational state II, where *Met80* decoordinates and is presumably replaced by a molecule of  $\text{H}_2\text{O}$ , is becoming more significant and dominant at lower pH. Consequently, the *heme* pocket is more exposed to the solvent providing a slightly higher hydrophobic character to the protein and probably favoring protein–protein interactions that make possible the formation of multi-layers on the electrode surface.

We next turn to exploring the immobilization of cyt-c at different pH values by cyclic voltammetry and its electrochemical response, as depicted in Fig. 4. Fig. 4A and B show an





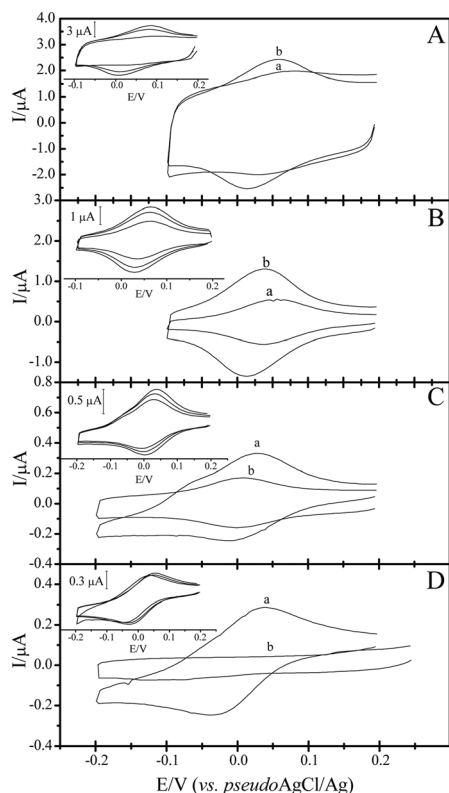


Fig. 4 Cyclic voltammetric profiles of 0.162 mM cyt-c/SPGE in 0.1 M PBS before (trace a) and after the immobilization procedure at 50 mV s<sup>-1</sup> (trace b) at different pH values: 2.0 (A), 3.0 (B), 4.0 (C) and 7.0 (D). Always shown the 3<sup>rd</sup> stable scan. Inset figures show the 1<sup>st</sup>, 50<sup>th</sup> and 100<sup>th</sup> scans from the immobilization procedure at 100 mV s<sup>-1</sup> at pH 2.0, 3.0, 4.0 and 7.0.

increased electrochemical profile after the immobilization process (curve b) compared to the third cycle of CV response when the protein is in solution (curve a), indicating that at these pH values, 2.0 and 3.0, the protein is adsorbed and remains almost unaltered in terms of its conformation at the electrode surface.

Furthermore, under the same experimental conditions as those applied in Fig. 4A and B, the adsorbed protein at pH 4.0 (Fig. 4C) shows that after the immobilization process (curve b) the CV response is lower than that observed in the third scan before immobilization (curve a). Also note that the redox peaks related principally to II-O and in a lesser manner to II-R clearly observed at this pH (curve a) are discarded in the voltammetric signature of adsorbed cyt-c, suggesting that this conformation is less probable than the native one. Unfortunately, there was no evidence for the electrochemical response of the adsorbed cyt-c after cycling at pH 7.0 due to probably a less favourable interaction with the electrode surface (Fig. 4D). The surface coverage ( $\Gamma$ ) of the protein can be estimated according to the following Laviron equation (eqn (1)):

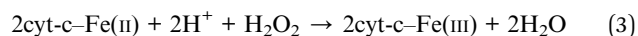
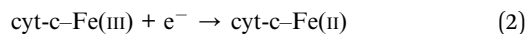
$$I_p = n^2 F^2 A \Gamma / 4RT = nFQv/4RT \quad (1)$$

where  $\Gamma$  (mol cm<sup>-2</sup>) is the average amount of adsorbed cyt-c on the electrode surface,  $A$  is the electrode area (cm<sup>2</sup>),  $n$  is the

number of electron transferred,  $Q$  is the charge involved in the reaction and  $F$  is Faraday's constant. Using a surface coverage calculation method,<sup>30</sup> at a scan rate of 50 mV s<sup>-1</sup>, a coverage of cyt-c gave rise to values of  $4.44 \times 10^{-11}$  mol cm<sup>-2</sup>,  $3.39 \times 10^{-11}$  mol cm<sup>-2</sup> and  $4.31 \times 10^{-12}$  mol cm<sup>-2</sup> at pH 2.0, 3.0 and 4.0, respectively. Coverage values denote multilayers of adsorbed cyt-c on the SPGE platform, when considering that for a theoretical monolayer of cyt-c when using a SAM-modified electrode the coverage should be  $1.40 \times 10^{-12}$  mol cm<sup>-2</sup>,<sup>31,32</sup> indicating that our measured surface coverage of cyt c is lower as the pH value increases. These results are in agreement with the fact that at low pH values the ET process is highly controlled by adsorption. In contrast, no redox peaks could be observed for the adsorption experiments carried out at pH 7.0 (as shown in Fig. 4D) meaning that the N conformation present at this physiological pH is not prone to adsorb largely on the surface of the electrode. Nevertheless, the presence of the adsorbed protein was proved by the observation of catalytic activity towards the addition of H<sub>2</sub>O<sub>2</sub> (Fig. 6).

### 3.3. Peroxidase activity of cyt-c immobilized on SPGE

The structural similarities of cyt-c with the family of peroxidases, the enzyme that makes the catalysis of H<sub>2</sub>O<sub>2</sub>, provide cyt-c with an intrinsic activity to convert H<sub>2</sub>O<sub>2</sub> to H<sub>2</sub>O, as described in the following equations (eqn (2) and (3)):



The response of cyt-c immobilized on the SPGE towards the effect of increasing amounts of H<sub>2</sub>O<sub>2</sub> was investigated by cyclic voltammetry in order to study the oxidative modification induced. Although the literature reports on the possible intervention of residual metals and enzymes to catalyze a range of side-reactions and produce non-specific oxidative damage *via* radical production, here the protein immobilization procedure prevented metals or impurities such as protein oligomers to be present in the experiments.<sup>33</sup> Due to this, it is surmised that these assays evidence the effect of the oxidative modification of cyt-c due to the interaction with the Fe in the *heme* pocket and the H<sub>2</sub>O<sub>2</sub> following catalysis of Fenton reaction. The *pseudoAg/AgCl* reference electrode of the SPGE was found to be stable over the timescale of the electrochemical experiments. The effect on the reference electrode stability due to the oxidizing conditions was discarded since a very well-defined reversible ET of the ferrocyanide/ferrocyanide redox couple remained unchangeable to the addition of H<sub>2</sub>O<sub>2</sub> for the same H<sub>2</sub>O<sub>2</sub> concentrations tested. However, from a biochemical point of view, the oxidative modification of cyt-c by H<sub>2</sub>O<sub>2</sub> has been studied extensively. For example, Kang and co-workers have shown the cyt-c oligomerization caused by the protein damage *via* carbonyl derivative generation and dityrosine bond formation in the presence of H<sub>2</sub>O<sub>2</sub>.<sup>33</sup> The oxidative damage of H<sub>2</sub>O<sub>2</sub>-sensitive amino acids (*Met*, *His* and *tyrosine*) is caused by free radicals generated by a mixture of a Fenton reaction of the free iron released from the oxidative-damaged protein and its peroxidase activity in the



presence of  $\text{H}_2\text{O}_2$ .<sup>33,34</sup> The oxidative damage to proteins has been widely reported to be produced by the generation of hydroxyl radicals and therefore prompting a broad number of covalent modifications at proteins.<sup>35–41</sup>

Fig. 5A shows the steady-state current response to five successive additions of 10  $\mu\text{L}$ , 0.2 M of  $\text{H}_2\text{O}_2$  into 2 mL of 0.1 M PBS pH 2.0 subjected to continuous stirring. The  $\text{H}_2\text{O}_2$  concentration in the bulk solution changes about 1 mM for each injection. The catalytic  $I_{\text{pc}}$  was measured at a potential of  $-0.5$  V (vs. *pseudo*Ag/AgCl) and it was found to increase steeply up to a “plateau” after 10 s. In Fig. 5B, the reciprocal of the catalytic  $I_{\text{pc}}$  was plotted vs. the reciprocal of the concentration of the substrate, in order to calculate the enzyme–substrate kinetics by using the Lineweaver–Burk plot,<sup>40,42</sup> as the inverse of the intercept of this plot, 14.8  $\mu\text{A}$ , corresponded to the  $i_{\text{max}}$ , and from the slope the Michaelis–Menten constant ( $K_{\text{m}}$ ),  $25 \pm 4$  mM, can be obtained for pH 2.0. Similarly, the peroxidase activity for cyt-c adsorbed at the SPGE was compared at other pH values, 3.0 and 7.0, as it is depicted in Fig. 6, with the same successive stepwise injections of  $\text{H}_2\text{O}_2$  to PBS solutions.  $K_{\text{m}}$  values were calculated by using the Lineweaver–Burk method and resulted to be  $98 \pm 12$  mM (pH 3.0) and  $230 \pm 30$  mM (pH 7.0), denoting a lower catalytic response or affinity of cyt-c towards the oxidation of  $\text{H}_2\text{O}_2$  probably due either to the more folded conformational state of the protein or low protein immobilised on the SPGE surface as physiological pH is reached.

Kinetics of the peroxidase activity of cyt-c adsorbed on the surface was satisfactorily studied under different pH values. Similar responses were obtained by Scheller and co-workers when they applied chronoamperometry at 0 V to their cyt-c

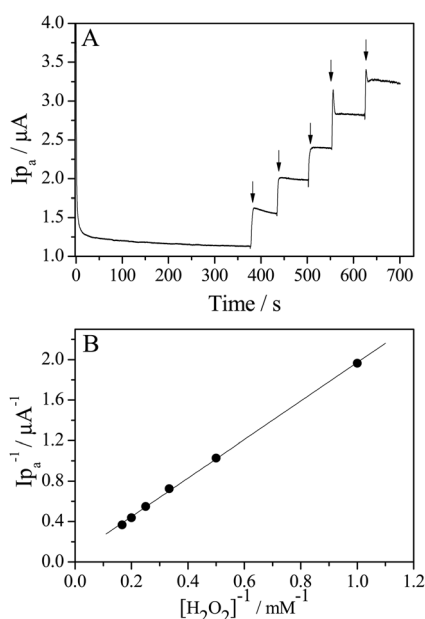


Fig. 5 (A) Catalytic response for adsorbed cyt-c/SPGEs at 0.1 M PBS pH 2.0 at  $-0.5$  V (vs. *pseudo*Ag/AgCl) with increasing amounts of  $\text{H}_2\text{O}_2$ . The arrows mark the points when the  $\text{H}_2\text{O}_2$  aliquot was added. (B) Lineweaver–Burk plot was used to yield the  $K_{\text{m}}$  and  $i_{\text{max}}$  parameters.

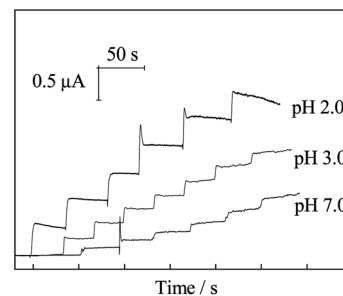


Fig. 6 Steady-state current intensity response of cyt-c immobilized on the SPGE following successive injections of 1 mM bulk concentration of  $\text{H}_2\text{O}_2$  into PBS solution pH 2.0, 3.0 and 7.0.

immobilized by polishing a colloidal gold modified carbon paste electrode on a plane glass surface with a drop of 4% cyt-c solution.<sup>43</sup> Wang and Waldeck<sup>40</sup> found similar  $K_{\text{m}}$  (7.9 mM) for pH 3.0 and 144 mM for pH 7.0 when cyt-c was adsorbed at carboxylic acid-terminated and hydroxyl-terminated SAMs on gold electrodes. At pH 2.0 the SPGE/cyt-c electrode exhibits a higher affinity to  $\text{H}_2\text{O}_2$  as the protein is presumably partially unfolded and then the *heme* pocket is more exposed.

## 4. Conclusions

SPGEs have been shown to be explored as novel platforms with unique properties due to the oxygenated species that allow the deeper study of biological aspects of cyt-c regarding the structure and function without the need for electrode surface modification as is commonly undertaken in the literature and consequently presents an easy and rapid experimental design. The signal-to-noise ratio presented in the CVs indicates clearly the utility of these electrodes for this purpose. We have examined the effect of pH on the electrochemical response of the ET process of cyt-c even under very extreme acidic and alkaline conditions. Furthermore, and according to the literature, it can be concluded that the reversible behaviour observed for cyt-c at pH 2.0 is caused by a high buffer concentration, while the impeded electron transfer that occurs at pH values higher than 8.0 can be due to electrostatic impediments. It has also been shown the striking co-existence of two conformations of cyt-c at pH values between 3.5 and 4.0 as means of a shoulder at moderate scan rates and a clear apparition of a “second pair of redox peaks” at low scan rates at slightly more negative potentials. Peroxidase activity of the immobilized cyt-c/SPGE was satisfactorily studied for the response to  $\text{H}_2\text{O}_2$  under different pH conditions exhibiting a higher response at pH 2.0 due to a considerable exposition of the *heme* pocket.

Our electrochemical approach for the characterization of the electron transfer of cyt-c shows relevant applications in terms of studying the effects that the oxidative stress agents can produce on electrochemical responses of proteins. For example, oxidation or nitration of cytochrome can notably alter its function and structure with consequences in electron transfer impediments, immobilization effectiveness and biosensing. The present findings will help understand the fundamentals of



interfacial redox processes, and may contribute to improve the performance of biosensors, bioelectronics, and biofuel cells.

## Acknowledgements

Authors would like to thank Prof. Aldaz for his fruitful contribution to the discussion of these results. Financial support from The Ministry of Science and Technology (project CTQ2010-18570) is gratefully acknowledged.

## References

- 1 J. Hirst, *Biochem. J.*, 2010, **425**, 327.
- 2 M. W. Fariss, C. B. Chan, M. Patel, B. Van Houten and S. Orrenius, *Mol. Interventions*, 2005, **5**, 94.
- 3 F. L. Rodkey and E. G. Ball, *J. Biol. Chem.*, 1950, **182**, 17.
- 4 R. E. Dickerson and R. Timkovick, Cytochromes c, in *The Enzymes*, ed. P. D. Boyer, Academic Press Inc., London, 3rd edn, 1975, vol. 11, p. 397.
- 5 P. X. Qi, R. A. Beckman and A. J. Wand, *Biochemistry*, 1996, **35**, 12275.
- 6 G. R. Moore and G. W. Pettigrew, in *Cytochromes c. Evolutionary, structural, and physicochemical aspects*, Springer-Verlag, Berlin, 1990.
- 7 M. Ohgushi and A. Wada, *FEBS J.*, 1983, **164**, 21.
- 8 Y. Goto, Y. Hagihara, D. Hamada, M. Hoshino and I. Nishii, *Biochemistry*, 1993, **32**, 11878.
- 9 Y. Goto and S. Nishikiori, *J. Mol. Biol.*, 1991, **222**, 679.
- 10 H. Christensen and R. H. Pain, *Eur. Biophys. J.*, 1991, **19**, 221.
- 11 G. Battistuzzi, C. A. Bortolotti, M. Bellei, G. Di Rocco, J. Salewski, P. Hildebrandt and M. Sola, *Biochemistry*, 2012, **51**, 5967.
- 12 A. Naeem and R. Hasan Khan, *Int. J. Biochem. Cell Biol.*, 2004, **36**, 2281.
- 13 A. A. Moosavi-Movahedi, J. Chamani, H. Ghourchian, H. Shafiey, C. M. Sorenson and N. Sheibani, *J. Protein Chem.*, 2003, **22**, 23.
- 14 F. Marken, C. A. Paddon and D. Asogan, *Electrochem. Commun.*, 2002, **4**, 62.
- 15 A. K. Abass and J. P. Hart, *Electrochim. Acta*, 2001, **46**, 829.
- 16 S.-F. Ding, W. Wei and G.-C. Zhao, *Electrochem. Commun.*, 2007, **9**, 2202.
- 17 L. Zhu, D. Sun, T. Lu, C. Cai, C. Liu and W. Xing, *Sci. China, Ser. B: Chem.*, 2007, **50**, 304.
- 18 C. Lei, F. Lisdat, U. Wollenberger and F. W. Scheller, *Electroanalysis*, 1999, **11**, 274.
- 19 M. Gómez-Mingot, J. Iniesta, V. Montiel, R. O. Kadara and C. E. Banks, *Analyst*, 2011, **136**, 2146.
- 20 H. A. Theorell and A. Akesson, *J. Am. Chem. Soc.*, 1941, **63**, 1804.
- 21 Y. P. Myer, L. H. MacDonald, B. C. Verma and A. Pande, *Biochemistry*, 1980, **19**, 199.
- 22 Y. P. Myer, A. F. Saturno, B. C. Verma and A. Pande, *J. Biol. Chem.*, 1980, **254**, 11202.
- 23 S. Monari, D. Millo, A. Ranieri, G. Di Rocco, G. van der Zwan, C. Gooijer, S. Peressini, C. Tavagnacco, P. Hildebrandt and M. Borsari, *J. Biol. Chem.*, 2010, **15**, 1233.
- 24 L. Banci, I. Bertini, G. Cavallaro and C. Luchinat, *J. Biol. Chem.*, 2002, **7**, 416.
- 25 W. Qin, R. Sanishvili, B. Plotkin, A. Schejter and E. Margoliash, *Biochim. Biophys. Acta*, 1995, **1252**, 87.
- 26 J. B. Wooten, J. S. Cohen, I. Vig and A. Schejter, *Biochemistry*, 1981, **20**, 5394.
- 27 E. Laviron, *J. Electroanal. Chem.*, 1979, **101**, 19.
- 28 R. Schweitzer-Stenner, R. Shah, A. Hagarman and I. Dragomir, *J. Phys. Chem. B*, 2007, **111**, 9603.
- 29 T. Pineda, J. M. Sevilla, A. J. Román and M. Blázquez, *Biochim. Biophys. Acta*, 1997, **1343**, 224.
- 30 E. Laviron, *J. Electroanal. Chem.*, 1979, **100**, 263.
- 31 L. Zhang, *Biosens. Bioelectron.*, 2008, **23**, 1610.
- 32 R. E. Dickerson, T. Tanako, D. Eisenberg, O. B. Kallai, L. Samson, A. Cooper and E. Margoliash, *J. Biol. Chem.*, 1971, **246**, 1511.
- 33 N. H. Kim, M. S. Jeong, S. Y. Choi and J. H. Kang, *Mol. Cells*, 2006, **22**, 220.
- 34 S. Raha and B. H. Robinson, *Trends Biochem. Sci.*, 2000, **25**, 502.
- 35 M. J. Davies, *Biochim. Biophys. Acta*, 2005, **1703**, 93.
- 36 K. Habermüller, M. Mosbach and W. Schuhmann, *Fresenius' J. Anal. Chem.*, 2000, **366**, 560.
- 37 P. K. Witting, A. G. Mauk and P. A. Lay, *Biochemistry*, 2002, **41**, 11495.
- 38 S. Y. Qian, Y. R. Chen, L. J. Deterding, Y. C. Fann, C. F. Chignell, K. B. Tomer and R. P. Mason, *Biochemistry*, 2002, **363**, 281.
- 39 A. K. Yagati, T. Lee, J. Min and J.-W. Choi, *Colloids Surf., B*, 2012, **92**, 161.
- 40 L. Wang and D. H. Waldeck, *J. Phys. Chem. C*, 2008, **112**, 1351.
- 41 M. Gómez-Mingot, L. A. Alcaraz, J. Heptinstall, A. Donaire, M. Piccioli, V. Montiel and J. Iniesta, *Arch. Biochem. Biophys.*, 2013, **529**, 26.
- 42 R. A. Kamin and G. S. Wilson, *Anal. Chem.*, 1980, **52**, 1198.
- 43 H. Ju, S. Liu, B. Ge, F. Lisdat and F. W. Scheller, *Electroanalysis*, 2002, **14**, 141.

